DOI: 10.1002/anie.201001524

Biogenic Nanoparticles

In Vivo Synthesis of Diverse Metal Nanoparticles by Recombinant *Escherichia coli***

Tae Jung Park, Sang Yup Lee, Nam Su Heo, and Tae Seok Seo*

Nanometer-scale metal particles are finding many applications in the fields of biology and nanotechnology owing to their unique optical and magnetic properties. Phytochelatin (PC) and other metal-binding proteins have an ability to bind heavy metals and have been used for heavy-metal removal. Thus, we reasoned that they might be employed for the synthesis of metal nanoparticles (NPs). Herein, we report the in vivo biosynthesis of diverse NPs by recombinant *Escherichia coli* expressing phytochelatin synthase (PCS) and/or metallothionein (MT). NPs of various metal elements, including semiconducting, alkali-earth, magnetic, and noble metals and rare-earth fluorides, could be synthesized in *E. coli*. The size of NPs could be tuned on the nanoscale by changing the concentration of metal ions in the medium. Thus, the controlled synthesis of NPs with desirable characteristics for in vitro assays and cellular imaging was possible. Paramagnetic NPs could also be synthesized by using the same system. The strategy of employing recombinant *E. coli* as an NP factory is generally applicable for the combinatorial synthesis of diverse NPs with a wide range of characteristics.

Metal NPs exhibit unique optical, electronic, and magnetic properties, which depend on their composition, size, and structure, and have therefore been explored extensively for various applications in bio- and nanotechnology.[1] Several physicochemical processes involving reactions at high temperatures in organic solvents have been employed for the synthesis of these metal NPs.[2] In nature, uni- and multicellular organisms are capable of reducing and accumulating metal ions as detoxification and homeostasis mechanisms upon their exposure to metal-ion solutions.[3–6] For example, CdS quantum crystallites of 2–6 nm in diameter were found to be synthesized intracellularly in *Candida glabrata*, *Schizosaccharomyces pombe*, and engineered *E. coli*.[3,4] In another example, the fungus *Verticillium* sp. was able to synthesize gold NPs of 20 nm in diameter by reducing aqueous $AuCl_4^-$ ions.[6] Also, it is known that 20–30 nm Fe_3O_4 magnetite nanocrystals can be synthesized by the magnetosome of *Magnetospirillum magnetotacticum*.[7,8] These examples demonstrate that microbes can be employed as a factory for metal-NP synthesis.

Although the exact mechanisms and identities of associated microbial proteins for metal-NP synthesis are not clear, two cysteine-rich, heavy-metal-binding biomolecules, PC and MT, have been relatively well characterized.[9–12] PCs are oligoglutathione peptides of varying sizes that are synthesized by PCS and that can form metal complexes with Cd, Cu, Ag, Pb, and Hg,[9,10] whereas MTs are gene-encoded proteins capable of directly binding Cu, Cd, and Zn.[10–12] Recently, the in vivo synthesis of CdS nanocrystals by recombinant *E. coli* expressing the *S. pombe* PCS gene and the γ-glutamylcysteine synthetase gene was reported.[4] However, the versatile capabilities of PC and MT to bind various metal ions and to form NPs have not been fully exploited.

Herein, we report a general strategy for the in vivo synthesis of diverse NPs by using recombinant *E. coli* expressing *Arabidopsis thaliana* PCS (AtPCS) and/or *Pseudomonas putida* MT (PpMT). Various metals, including semiconducting (Cd, Se, Zn, Te), alkali-earth (Cs, Sr), magnetic (Fe, Co, Ni, Mn), and noble (Au, Ag) metals and rare-earth fluorides (Pr, Gd), were incubated in assorted combinations with the recombinant *E. coli* cells for the in vivo synthesis of the corresponding metal NPs. The resulting NPs were analyzed for their optical, magnetic, and physicochemical properties. Recombinant *E. coli* strains expressing AtPCS, PpMT, or both AtPCS and PpMT were also designed and examined for their ability to synthesize diverse metal NPs. Quantum dots (QDs), fluorescent semiconducting material, were used as an example in experiments to tune the sizes of NPs by varying the concentration of the metal ion in the medium. Finally, functionalized QDs were applied to the in vitro conjugation of biomaterials and cellular-imaging analysis.

In vivo NP synthesis in recombinant *E. coli* is described schematically in Figure S1 of the Supporting Information.

[*] Dr. T. J. Park, Prof. S. Y. Lee, N. S. Heo, Prof. T. S. Seo
Department of Chemical and Biomolecular Engineering
BioProcess Engineering Research Center
Center for Systems and Synthetic Biotechnology
Institute for the BioCentury, KAIST
335 Gwahangno, Yuseong-gu, Daejeon 305-701 (Republic of Korea)
Fax: (+82) 42-350-8800
E-mail: leesy@kaist.ac.kr
Homepage: http://mbel.kaist.ac.kr
Prof. S. Y. Lee
Department of Bio and Brain Engineering, Department of Biological Sciences, Bioinformatics Research Center, KAIST
335 Gwahangno, Yuseong-gu, Daejeon 305-701 (Republic of Korea)

[**] This research was supported by the WCU (World Class University) program through the National Research Foundation of Korea funded by the Ministry of Education, Science and Technology (R322009000101420), and in part by the IT Leading R&D Support Project from the Ministry of Knowledge Economy through KEIT. Further support by the KAIST Institute for the BioCentury is appreciated. We thank Dr. Z. W. Lee and H. J. Cho (Korea Basic Science Institute, Korea) for assistance with confocal microscopy and TEM imaging, respectively. We also thank Dr. J. H. Yoo (National NanoFab Center, Korea) for assistance with TEM and EDX analysis and Prof. G. Choi (KAIST, Korea) for kindly providing us with the cDNA library of *A. thaliana*.

Supporting information for this article is available on the WWW under http://dx.doi.org/10.1002/anie.201001524.

Plasmids pTJ1-AtPCS, pTJ1-PpMT, pACtac-PpMT, and pTJ11-PpMT-n-AtPCS were constructed for the expression of the AtPCS and PpMT genes, either alone or together. The metal ions were added in various combinations at concentrations of 0.5, 1.0, 2.0, 3.0, and 5.0 mM each (see Tables S1 and S2 in the Supporting Information). The recombinant *E. coli* strains DH5α (pTJ1-AtPCS) and DH5α (pTJ1-PpMT) were able to synthesize semiconducting NPs inside the cells when they were incubated with various combinations of Cd, Se, Zn, and Te (each 5.0 mM). The NPs synthesized in this way were characterized by transmission electron microscopy (TEM) and high-resolution TEM (HRTEM). The semiconducting CdZn, CdSe, CdTe, and SeZn NPs synthesized in *E. coli* DH5α (pTJ1-AtPCS) exhibited well-defined crystalline structures with average diameters of (10.01 ± 0.97), (5.01 ± 0.89), (7.01 ± 0.66), and (3.92 ± 0.35) nm and interplanar distances of (4.40 ± 0.34), (3.51 ± 0.18), (3.00 ± 0.12), and (2.82 ± 0.23) Å, respectively (Figure 1 a–d). They showed {111} face-centered-monoclinic, {111} cubic, {102} hexagonal, and {012} monoclinic structures, respectively.[13] The CdZn, CdSe, CdTe, and SeZn NPs synthesized in *E. coli* DH5α (pTJ1-PpMT) expressing MT also exhibited well-defined crystalline structures, with interplanar lattice distances of (2.96 ± 0.21), (2.85 ± 0.13), (3.69 ± 0.38), and (3.25 ± 0.21) Å, and showed {221} monoclinic, {121} orthorhombic, {111} cubic, and {111} cubic structures, respectively (Figure 1 e–h). The average diameters of these CdZn, CdSe, CdTe, and SeZn NPs were (10.35 ± 0.68), (4.99 ± 0.69), (5.83 ± 1.60), and (3.95 ± 1.12) nm, respectively.

The CdTe and SeZn NPs exhibited diverse sizes and atypical shapes. These results demonstrate that various semiconducting nanocrystallites can be synthesized in vivo by PC (synthesized by AtPCS) and PpMT expressed in *E. coli* cells. The size and d-lattice structure of NPs synthesized in vivo by PC and MT were different, which suggests that the characteristics of metal binding and assembly are different for PC and MT, as reported previously.[9–11,14] MT has been shown to have a greater binding affinity for Cu than for Cd or Zn.[12] Also, it has been reported that one Cd ion is bound to two and three cysteine residues in PC and MT, respectively.[9,14] Thus, we reasoned that the coexpression of AtPCS and PpMT in *E. coli* might enable the synergistic synthesis of more-diverse metal NPs.

For the coexpression of AtPCS and PpMT, two different expression systems involving one (pTJ11-PpMT-n-AtPCS) and two plasmids (pTJ1-AtPCS and pACtac-PpMT) were employed. Recombinant *E. coli* strains were incubated with various combinations of metal ions, including semiconductor metals (Cd, Se, Zn, Te), noble metals (Au, Ag), alkali-earth metals (Cs, Sr), rare-earth fluorides (Pr, Gd), and magnetic metals (Fe, Co, Ni, Mn). Cells coexpressing PpMT and AtPCS also accumulated NPs. CdZn, CdSe, CdTe, and SeZn NPs showed well-defined crystalline structures with interplanar lattice distances of (2.82 ± 0.13), (3.51 ± 0.24), (3.22 ± 0.13), and (3.25 ± 0.19) Å, corresponding to {221} monoclinic, {111} cubic, {111} cubic, and {111} cubic-plane structures, respectively (Figure 1 i–l): typical structures for these NPs.[13] The size and d-lattice structure of CdSe NPs synthesized by PC–MT were similar to those of CdSe NPs obtained by AtPCS expression, whereas the size and d-lattice structure of SeZn NPs synthesized by PC-MT were similar to those of SeZn NPs obtained by PpMT expression. However, the CdZn and CdTe NPs showed different lattice structures from those obtained with either PC or MT. This result suggests that the AtPCS/PpMT coexpression approach has the potential to generate diverse metal NPs.

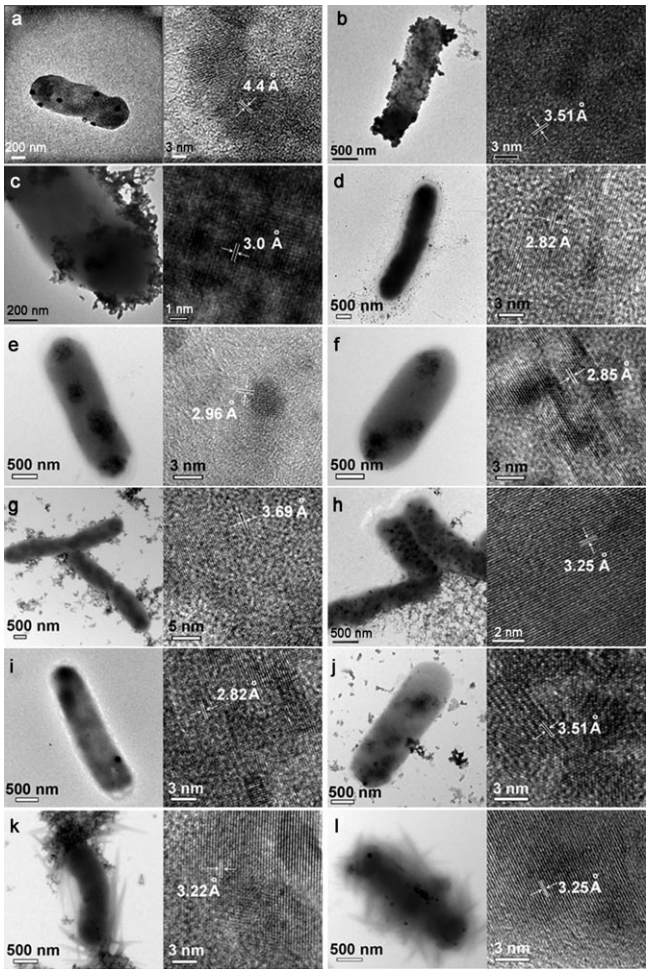

Figure 1. TEM images of various semiconducting NPs synthesized in vivo by recombinant *E. coli* cells incubated with the corresponding metal ions (5 mM each): a) CdZn, b) CdSe, c) CdTe, and d) SeZn NPs synthesized by recombinant *E. coli* cells expressing AtPCS; e) CdZn, f) CdSe, g) CdTe, and h) SeZn NPs synthesized by recombinant *E. coli* cells expressing PpMT; i) CdZn, j) CdSe, k) CdTe, and l) SeZn NPs synthesized by recombinant *E. coli* cells expressing both AtPCS and PpMT (one plasmid). The distance indicated on each HRTEM image is the interplanar distance of the NP lattice.

We used CdSe QDs as an example to compare the fluorescence emission intensities of nanoparticles obtained in various *E. coli* strains. The fluorescence emission intensity of CdSe QDs synthesized in recombinant cells coexpressing the AtPCS and PpMT by one- and two-plasmid systems was four times as high as that observed for CdSe QDs synthesized in cells expressing AtPCS or PpMT alone (see Figure S2 in the Supporting Information). This result suggests that the coexpression system enabled a more efficient synthesis of CdSe NPs. We analyzed the amounts of PC synthesized in three

recombinant *E. coli* strains expressing AtPCS or both PpMT and AtPCS with one- and two-plasmid systems (see Figure S3 in the Supporting Information). As the one- and two-plasmid systems expressing both AtPCS and PpMT showed similar capabilities of NP synthesis, the former system was selected for further studies, as the expression levels of AtPCS and PpMT are subject to more variation when the two-plasmid system is employed owing to the use of two different replication origins.

By using recombinant *E. coli* DH5α harboring pTJ11-PpMT-n-AtPCS (hereafter EcMP), we examined the possibility of synthesizing various metal NPs. The EcMP cells were incubated with various combinations of metal ions, including semiconductor metals (Cd, Se, Zn, Te), rare-earth fluorides (Pr, Gd), alkali-earth metals (Cs, Sr), magnetic metals (Fe, Co, Ni, Mn), and noble metals (Au, Ag). As well as typical CdZn, CdSe, CdTe, and SeZn QDs, complex NPs, such as CdSeZn semiconducting nanocrystallites (Figure 2a), could

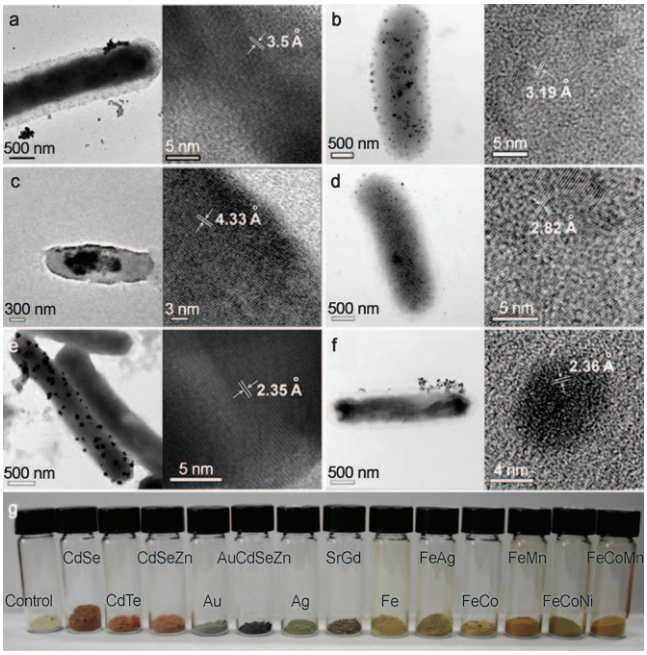

Figure 2. a–f) TEM images of various NPs synthesized in EcMP cells (the distance indicated on each HRTEM image is the interplanar distance of the NP lattice). New types of NPs, including CdSeZn (a), PrGd (b), CdCs (c), and FeCo (d), could be synthesized in recombinant *E. coli* expressing AtPCS and PpMT by incubating the cells with the corresponding metal ions (5 mM each). Also, Au (e) and Ag NPs (f) could be synthesized by incubating cells with Au (1.25 mM) and Ag ions (5 mM), respectively. g) Multicolored freeze-dried *E. coli* cells containing a variety of NPs. All NPs showed well-defined crystalline nanostructures.

be synthesized in EcMP cells. NPs of rare-earth metals (PrGd, Figure 2b) were also synthesized; PrGd nanoparticles showed an interplanar distance of (3.19 ± 0.10) Å and a {222} cubic structure. Furthermore, NP complexes of alkali-earth and rare-earth metals (SrGd and SrPr; see Figure S4 in the Supporting Information) were synthesized as new types of metal NPs with interplanar distances of (3.10 ± 0.07) and (3.47 ± 0.02) Å, respectively. Interestingly, NP complexes of semiconducting and alkali-earth metals (CdCs, Figure 2c) were also synthesized as a new type of metal NP.

Various ferromagnetic NPs could also be synthesized in this way. Magnetic NPs are known to be synthesized by the magnetosomes of magnetotactic bacteria.[8,15] Even in the absence of microbial magnetosomes, the metal-binding ability of MT and PC enabled the successful assembly of various ferromagnetic particles Fe–X (X = Ag, Mn, Co, Co/Ni, Co/Mn). As representative examples, HRTEM images of FeCo and FeCoNi NPs are shown in Figure 2d and Figure S5 of the Supporting Information, respectively. The FeCo NPs composed of magnetic metals exhibited well-defined crystalline structures with interplanar distances of (2.82 ± 0.05) Å. Furthermore, the diameter of FeCo metal NPs could be tuned from (3.02 ± 1.00) to (5.57 ± 1.04) nm by increasing the concentration of Fe^{2+} (or Fe^{4+}) and Co^{2+} metal ions from 0.5 to 2.0 mM (see Figure S6 and Table S2 in the Supporting Information).

Atypical podlike Au (Figure 2e; see also Figure S7 in the Supporting Information) and Ag nanocrystallites (Figure 2f) could also be synthesized in EcMP cells. When Au or Ag was provided, gold and silver NPs exhibiting interplanar distances of (2.35 ± 0.03) and (2.36 ± 0.05) Å, respectively, in the {111} direction were synthesized.

It is remarkable that the EcMP strain enabled MT and PC (synthesized by PCS) to function synergistically towards the enhanced nanostructure assembly of more-diverse metals. The distinct colors of the freeze-dried cells depended on the metal NPs accumulated within the cells (Figure 2g). The chemical compositions of these NPs were confirmed by energy-dispersive X-ray spectroscopy (EDX; see Figures S7–S9 in the Supporting Information). This study is the first demonstration of the use of engineered bacteria for the in vivo synthesis of a wide range of functional metal NPs.

We examined recombinant *E. coli* cells incubated with solutions of various combinations of metal ions (5.0 mM) by confocal fluorescence microscopy (Figure 3a–f). Semiconducting CdSe (Figure 3b–d) and CdTe (Figure 3e) NPs showed red fluorescence, whereas the novel SrGd NPs exhibited cyan and red mixed fluorescence (Figure 3f; see also Figure S10 in the Supporting Information). The SrGd NPs synthesized in recombinant *E. coli* cells were present in isolated and aggregated forms. In their isolated form, they exhibited cyan fluorescence, but upon aggregation they exhibited red fluorescence. The average diameters of the CdSe and CdTe NPs were approximately (5.10 ± 0.57) and (7.01 ± 0.82) nm, respectively. The novel PrGd, SrGd, and SrPr NPs synthesized by incubating cells with the corresponding metal-ion solutions (0.5, 1.0, or 2.0 mM) exhibited defined crystalline structures with average diameters of 3–10 nm (see Table S2 in the Supporting Information). However, these NPs obtained by incubation with combinations of Pr^{3+}, Gd^{3+}, and Sr^{2+} at a concentration of 5.0 mM each exhibited heterogeneous size distribution, ranging from several to hundreds of nanometers, and showed cyan–green and far-red fluorescence emission spectra at 460 nm in the case of PrGd and 420 and 720 nm in the case of SrGd and SrPr (see Figure S10 in the Supporting Information). The formation of NPs was con-

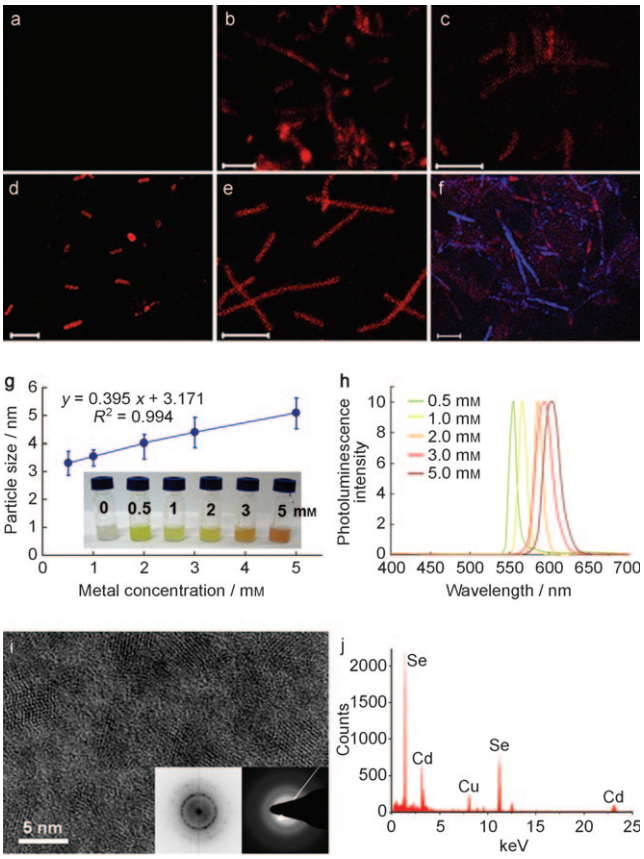

Figure 3. Optical and chemical properties of metal NPs synthesized in recombinant *E. coli* cells. a–f) Confocal fluorescence emission images recorded upon excitation at 488 nm with an Ar–Kr laser. An absence of metal-binding proteins in *E. coli* cells resulted in no fluorescence emission signal (a); recombinant *E. coli* cells accumulating CdSe NPs by the expression of AtPCS (b), PpMT (c), and AtPCS and PpMT (one-plasmid system; d) showed red fluorescence. Recombinant *E. coli* accumulating CdTe NPs by the expression of PpMT also exhibited red fluorescence (e). Recombinant *E. coli* accumulating SrGd NPs by the expression of AtPCS and PpMT (one-plasmid system) showed cyan–green fluorescence (f). The metal-ion concentration was 5 mM. Scale bars: 5 μm. g) Graph showing the correlation between the concentration of the metal-ion solution (0.5, 1.0, 2.0, 3.0, and 5.0 mM) and the size of the resulting CdSe nanoparticles with EcMP cells. An image of the purified CdSe NPs is shown in the inset. h) Fluorescence emission spectra of CdSe NPs in deionized water. i) HRTEM image of purified CdSe NPs from EcMP cells incubated with Cd and Se ions (each 5.0 mM). The electron-diffraction pattern is shown in the inset. j) EDX spectrum of purified CdSe NPs. The Cu peak is from the copper TEM grid.

firmed by UV/Vis absorption spectra, which showed peaks centered at about 250 and 280 nm (see Figures S11–S13 in the Supporting Information).

It is essential to be able to control the size of NPs if industrial applications are to be pursued. As the size of a QD affects its fluorescence characteristics, we examined the possibility of tuning the sizes of the CdSe NPs in EcMP cells by incubating the cells with Cd^{2+} and Se^{+} metal ions at different concentrations; we then analyzed approximately 50 particles by TEM. The CdSe NPs were purified by filtration through a membrane with 0.1 μm pores after cell disruption. By varying the concentration of the metal ions from 0.5 to 5.0 mM, the diameter of CdSe NPs could be tuned from (3.31 ± 0.43) to (5.10 ± 0.57) nm. Accordingly, these CdSe NPs exhibited several unique colors, depending on their size (Figure 3g). In a similar way, the diameter of CdZn NPs could be tuned from (3.02 ± 1.00) to (14.84 ± 1.02) nm (see Figure S14 in the Supporting Information). The fluorescence emission spectrum of the CdSe NPs was narrow and symmetric, with a full width at half maximum of 15–25 nm (Figure 3h); the spectral pattern was typical for QDs.

Surface characterization of the extracted CdSe NPs by mid-FTIR spectroscopy (1689, 1639, 1365, 1236, and 713 cm^{-1}; see Figure S15 in the Supporting Information) and FT Raman spectroscopy (3216, 2926, 1692, 1630, 1422, and 797 cm^{-1}; see Figure S16 in the Supporting Information) revealed that the CdSe NPs were surrounded by peptides, which are most likely MTs and PCs. The peptide coating of NPs is known to provide colloidal stability and NP biocompatibility.[16] New applications might be possible upon modification of the NPs with versatile functional groups.

For the preparation of pure metal NPs for chemical and optical analysis, the crude CdSe NPs isolated from *E. coli* cells incubated with Cd^{2+} and Se^{+} metal ions (5 mM each) were calcinated at 700 °C for 12 hours to remove organic materials coated on the surface. The purified CdSe NPs were visible to the naked eye as far-red-emitting NPs with an upconversion light source. HRTEM analysis of purified CdSe NPs showed that individual NPs were subspherical and oval-shaped with an average diameter of 5.10 nm (Figure 3i). Electron diffraction analysis showed diffuse ring patterns and crystal spots with a d spacing of (3.51 ± 0.24) Å, which indicated a randomly oriented, finely crystalline nanostructure (Figure 3i, inset). The presence of Cd and Se elements in the NPs was verified by the EDX spectrum (Figure 3j). The CdSe and CdZn NPs exhibited fairly broad bands centered at about 380 and 420 nm, respectively, in their UV/Vis absorption spectra (see Figure S17 in the Supporting Information). These bands were not observed in the negative control experiment, in which the sample was prepared with *E. coli* cells lacking metal-binding proteins, and the same NP synthesis and purification procedures were then carried out. Thus, the semiconductor CdSe NPs synthesized in recombinant *E. coli* cells were size-tunable and possessed chemical and optical characteristics comparable, if not identical, to those of chemically synthesized QDs.

Novel iron-based magnetic NPs synthesized by EcMP cells were characterized by vibrating sample magnetometer (VSM) analysis (see Figure S18a in the Supporting Information). We examined the ferromagnetic NPs, which showed different magnetization values depending on the chemical composition, and found that *E. coli* cells containing the FeCo/Ni and FeCo/Mn nanomagnetites showed unsaturated magnetization with an increasing magnetic field up to 15 kOe. Thus, these nanomagnetites demonstrated high paramagnetic characteristics. Since the VSM measurement was conducted with peptide-coated NPs in the cells, a simple purification procedure following sample preparation is sufficient for the isolation of nanomagnetites with great paramagnetic strength (see the Supporting Information). The magnetite-containing

E. coli cells could be separated simply by using an external magnet (see Figure S18b in the Supporting Information). These results indicate that paramagnetic NPs could be synthesized efficiently in recombinant *E. coli* for various applications, including biomolecular tagging, angiographic imaging, separation, and drug delivery.

As an example application of NPs synthesized in vivo, we carried out a functionalization assay and intracellular confocal imaging studies with CdSe QDs as in vitro labeling agents. The purified CdSe QDs were incubated with anti-rabbit immunoglobulin G (IgG) conjugated with fluorescein isothiocyanate (FITC) for 1 hour at room temperature. The fluorescence emission spectrum of IgG-conjugated CdSe QDs exhibited dual fluorescence peaks corresponding to FITC (conjugated with IgG) and CdSe QDs (Figure 4a), which suggests that FITC–IgG molecules were successfully tagged onto the QD surface. For the efficient delivery of QDs into live cells, the cell-penetrating peptide (CPP) GRKKRRQRRRPPQC, which is the transactivating transcriptional activator (TAT) of human immounodeficiency virus type 1,[17] was immobilized on the surface of QDs. The CPP-functionalized QDs were then incubated with human fibroblast cells. As shown in Figure 4b–e, the CPP-functionalized QDs were localized to the nuclei of fibroblast cells (Figure 4b). Nuclear Hoechst staining was performed for comparison (Figure 4c). These results indicate that the QDs synthesized in recombinant *E. coli* can be used as ex vivo and in vitro fluorescent probes for biomolecular conjugation, imaging, and targeted delivery.

In summary, we have developed a recombinant *E. coli* system expressing PCS and/or MT for the in vivo synthesis of various metal NPs, including NPs never synthesized before by chemical methods. Furthermore, the coexpression of PCS and MT in *E. coli* resulted in the enhanced assembly of diverse metal elements into highly ordered NPs. The size of the metal NPs could be controlled by adjusting the concentrations of the supplied metal ions. As the high-cell-density culture of *E. coli* has been well established,[18] the efficient and cost-effective production of various metal NPs would not be a difficult task. The engineered *E. coli* system reported herein should be broadly applicable to the in vivo synthesis of metal NPs of interest with tailored optical, electronic, chemical, and magnetic properties.

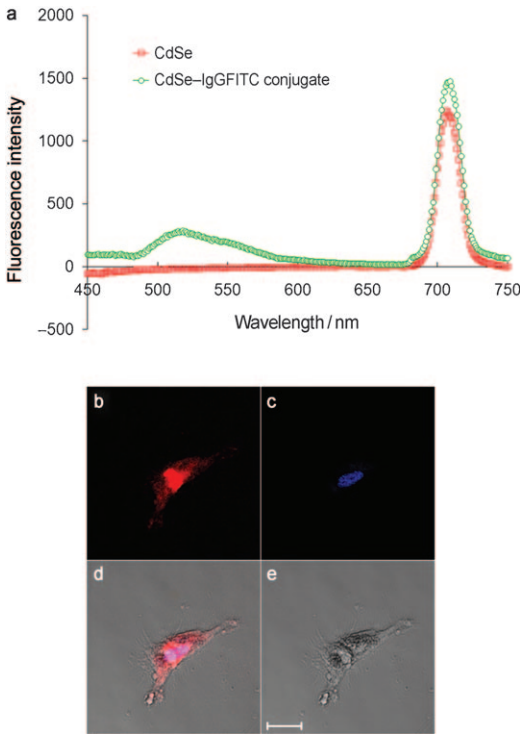

Figure 4. Functionalization of the QDs synthesized in vivo. a) Fluorescence emission scanning spectra of unfunctionalized CdSe QDs (red circles) and CdSe QDs after in vitro functionalization with anti-rabbit IgG conjugated with FITC (green circles). b) Cellular fluorescence image (excitation at 488 nm and emission at 560–615 nm) after treatment with CdSe QDs conjugated with the CPP TAT, which appears red. c) Confocal fluorescence image (excitation at 650 nm and emission at 670–700 nm) after simple vital nuclear staining with Hoechst dye, which appears blue. d) Multifluorescence image created by the integration of (b) and (c). e) Optical microscopic image of a human fibroblast cell. Scale bar: 50 μm.

Received: March 14, 2010
Published online: August 18, 2010

Keywords: bacteria · biotechnology · in vivo synthesis · metal-binding proteins · metal nanoparticles

[1] a) M. Bruchez, Jr., M. Moronne, P. Gin, S. Weiss, A. P. Alivisatos, *Science* **1998**, *281*, 2013–2016; b) W. C. Chan, S. Nie, *Science* **1998**, *281*, 2016–2018; c) D. J. Milliron, S. M. Hughes, Y. Cui, L. Manna, J. Li, L. W. Wang, A. P. Alivisatos, *Nature* **2004**, *430*, 190–195; d) I. L. Medintz, H. T. Uyeda, E. R. Goldman, H. Mattoussi, *Nat. Mater.* **2005**, *4*, 435–446.

[2] a) C. B. Murray, D. J. Norris, M. G. Bawendi, *J. Am. Chem. Soc.* **1993**, *115*, 8706–8715; b) C. B. Murray, C. R. Kagan, M. G. Bawendi, *Science* **1995**, *270*, 1335–1338; c) Q. Peng, Y. Dong, Y. Li, *Angew. Chem.* **2003**, *115*, 3135–3138; *Angew. Chem. Int. Ed.* **2003**, *42*, 3027–3030; d) Y. Sun, Y. Xia, *Science* **2002**, *298*, 2176–2179.

[3] C. T. Dameron, R. N. Reese, R. K. Mehra, A. R. Kortan, P. J. Carroll, M. L. Steigerwald, L. E. Brus, D. R. Winge, *Nature* **1989**, *338*, 596–597.

[4] S. H. Kang, K. N. Bozhilov, N. V. Myung, A. Mulchandani, W. Chen, *Angew. Chem.* **2008**, *120*, 5264–5267; *Angew. Chem. Int. Ed.* **2008**, *47*, 5186–5189.

[5] M. Labrenz, G. K. Druschel, T. Thomsen-Ebert, B. Gilbert, S. A. Welch, K. M. Kemner, G. A. Logan, R. E. Summons, G. D. Stasio, P. L. Bond, B. Lai, S. D. Kelly, J. F. Banfield, *Science* **2000**, *290*, 1744–1747.

[6] P. Mukherjee, A. Ahmad, D. Mandal, S. Senapati, S. R. Sainkar, M. I. Khan, R. Ramani, R. Parischa, P. V. Ajayakumar, M. Alam, M. Sastry, R. Kumar, *Angew. Chem.* **2001**, *113*, 3697–3701; *Angew. Chem. Int. Ed.* **2001**, *40*, 3585–3588.

[7] A. Bharde, D. Rautaray, V. Bansal, A. Ahmad, I. Sarkar, S. M. Yusuf, M. Sanyal, M. Sastry, *Small* **2006**, *2*, 135–141.

[8] R. Sriprang, M. Hayashi, H. Ono, M. Takagi, K. Hirata, Y. Murooka, *Appl. Environ. Microbiol.* **2003**, *69*, 1791–1796.

[9] K. Hirata, N. Tsuji, K. Miyamoto, *J. Biosci. Bioeng.* **2005**, *100*, 593–599.

[10] C. Cobbett, P. Goldsbrough, *Annu. Rev. Plant. Biol.* **2002**, *53*, 159–182.

[11] N. J. Robinson, S. K. Whitehall, J. S. Cavet, *Adv. Microb. Physiol.* **2001**, *44*, 183–213.

[12] P. Coyle, J. C. Philcox, L. C. Carey, A. M. Rofe, *Cell. Mol. Life Sci.* **2002**, *59*, 627 – 647.
[13] Powder Diffraction Data File 38 – 1364, Inorganic Phases, JCPDS International Centre for Diffraction Data, Swathmore, PA, 199.
[14] E. Grill, E.-L. Winnacker, M. H. Zenk, *Science* **1985**, *230*, 674 – 676.
[15] D. A. Bazylinski, R. B. Frankel, *Nat. Rev. Microbiol.* **2004**, *2*, 217 – 230.
[16] a) X. Michalet, F. F. Pinaud, L. A. Bentolila, J. M. Tsay, S. Doose, J. J. Li, G. Sundaresan, A. M. Wu, S. S. Gambhir, S. Weiss, *Science* **2005**, *307*, 538 – 544; b) F. Pinaud, D. King, H. P. Moore, S. Weiss, *J. Am. Chem. Soc.* **2004**, *126*, 6115 – 6123.
[17] a) A. D. Frankel, C. O. Pabo, *Cell* **1988**, *55*, 1189 – 1193; b) E. Vives, P. Brodin, B. Lebleu, *J. Biol. Chem.* **1997**, *272*, 16010 – 16017.
[18] S. Y. Lee, *Trends Biotechnol.* **1996**, *14*, 98 – 105.

